Optical properties of serpentine superlattices on GaAs vicinal substrates for quantum wire laser applications

Jong Chang Yi and Nadir Dagli
Electrical and Computer Engineering Department, University of California, Santa Barbara, California 93106

(Received 7 February 1992; accepted for publication 27 April 1992)

In this letter, the first detailed theoretical study of optical gain in serpentine superlattice quantum wire arrays grown on GaAs vicinal substrates is presented. In the calculations, the complex nature of the miniband structure due to coupling between wires and the valence band intermixing are taken into account. In addition to the ideal structure, the effects of imperfect Al segregation between GaAs wires and AlGaAs barriers are also investigated.

Recently, there have been significant efforts to study[1–4] and develop[5–8] quantum wires (QWR) for their interesting physical properties as well as their potential device applications.[9–11] In QWR, to observe significant quantum effects at room temperature, the carriers must be confined to regions less than about 100 Å in two dimensions.[3] One possibility to fabricate such QWR is using tilted superlattices (TSL).[7] These lateral superlattices are directly grown by sequential deposition of two materials of different compositions on an off-axis or vicinal GaAs substrate, on which uniform atomic steps are formed under proper growth conditions. The end result is an array of QWR with a period T. The period is determined by the substrate tilt angle, α, and monolayer thickness, d, which can be expressed[7] as $T=d/\tan\alpha$. For example, when α is 2°, T becomes 81 Å, and when α is 1.5°, T becomes 108 Å in AlGaAs system.

There is one practical difficulty in the fabrication of a TSL, however. To keep the growth interface vertical, one has to know the exact growth rates and keep them constant throughout the growth. Any deviation from the correct value would tilt the growth interface.[7] This difficulty can be circumvented if one deliberately varies the growth rate from less than the correct value to greater than the correct value.[12] Then one grows a superlattice with a curved growth interface as shown in Fig. 1. Somewhere within this so-called serpentine superlattice (SSL), one obtains a vertical interface, hence two-dimensional confinement as schematically indicated in Fig. 1. This approach enhances the uniformity of the array significantly and removes the precise growth rate control requirement. Although this is a drastic improvement over TSL, other difficulties in realizing SSL with optical properties superior to quantum wells remain. These are fluctuations in the widths of the wires and barriers and incomplete Al segregation. The aim of this letter is twofold. First optical properties of the ideal SSL are studied and compared with that of quantum wells of the same degree of confinement as in one of the cross-sectional dimensions of SSL. Next the effect of incomplete Al segregation, which is the main difficulty at the present time, is investigated.

In the analysis, first the energy band diagram of SSL is calculated by solving the Schrödinger equation using the finite-element method. For conduction band calculations a single band model is used which is shown to be a good approximation in the presence of thin barriers.[13] For valence band calculations a 4 band $k\cdot p$ analysis[14] is used to take into account the valence band mixing effects. In all the calculations finite potential barriers and periodic boundary conditions are utilized allowing the analysis of the infinite array of QWR in an SSL. Furthermore, the coupling between the wires due to their close spacing and finite barrier heights are taken into account. Once the E-k diagram is generated, density of state functions and other optical properties can be obtained.

The schematic cross-sectional profile of the SSL geometry is shown in Fig. 1. The curvature[12] of the growth interface provides vertical confinement. The degree of vertical confinement depends on the substrate tilt angle, α, the total thickness of the SSL, D_0, and the intentional variation of the growth rate, Δp. The shape of the vertical curved interface can be expressed as $y=\Delta p/(\tan\alpha\cdot D_0)z^2$. p, known as the tilt parameter, is defined as $p=m+n$, where m and n are the fractions of barrier and well material on a step. If the deposition or growth rate is adjusted such that $p=m+n=1$ the amount of material deposited per monolayer exactly covers a step and the interface between the

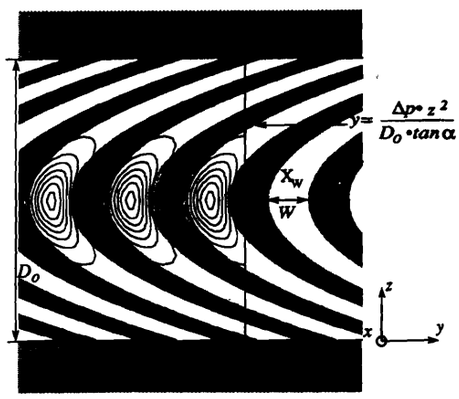

FIG. 1. Schematic cross-sectional profile of a SSL and its electron probability density for the lowest conduction band subband at zone center. The gray and white areas represent $Al_{0.5}Ga_{0.5}As$ and GaAs regions respectively. $W+S=T$ where T is the period of the superlattice.

 0003-6951/92/270219-03$03.00

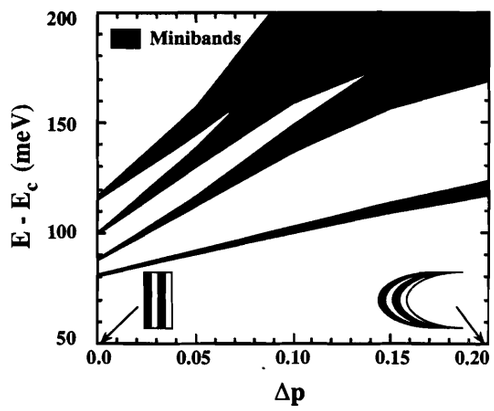

FIG. 2. Variation of the miniband spacings and widths as a function of the growth rate variation for a SSL with $x_b=0.5$, $x_c=0.50$, $W=S=54$ Å, $D_0=460$ Å as the growth rate varies up to $\pm 20\%$. Only four lowest minibands are plotted. E_c denotes the GaAs conduction band edge energy.

well and barrier material will grow vertically. If $p<1$ or $p>1$ interface will tilt one way or the other. $\Delta p=|p-1|$ indicates the intentional deviation from the nominal p value of 1 and determines the slope of the interface. Δp, α, and D_0 plus the Al contents in the wires, barriers and the claddings, x_w, x_b, and x_c, respectively, are the parameters that are available to optimize the structure.

Figure 2 shows the variation of the conduction band miniband spacings and widths of a SSL on 1.5° vicinal GaAs substrate, i.e., when $W=S=54$ Å. The tilt parameter p is varied up to $\pm 20\%$ and $x_w=0$, $x_b=x_c=0.5$, and $D_0=460$ Å. In this figure it is observed that individual eigenstates in the wires are broadened into minibands because the barrier between the wires is very thin resulting in coupling between the wires. When $\Delta p=0$ the well and barrier interfaces are vertical and the SSL is a quantum well array with additional weak vertical confinement. The subband spacing is very small due to weak vertical confinement. As Δp increases, the curvature of the interface increases and the vertical confinement becomes stronger. This increases the subband spacing between the lowest minibands. When Δp is 0.20, the miniband spacing between the two lowest energy levels becomes 46 meV. As Δp increases, however, the widths of the minibands also become broadened due to excessive coupling between the wires, and consequently, the energy minibands overlap with each other in the higher subbands.

The corresponding room temperature modal gain curves with an assumed Gaussian line shape function[3] of $\Delta E=6$ meV are shown in Fig. 3. The optical confinement is obtained by placing $Al_{0.7}Ga_{0.3}As$ optical cladding layers 0.1 μm above and below $Al_{0.5}Ga_{0.5}As$ layers on the top and bottom of SSL. The optical confinement factor required for modal gain calculations is obtained by calculating the overlap integral between the optical mode and the electronic wavefunction. In Fig. 3(a), the gain spectra are plotted for various Δp values when the injected surface carrier density, n_s, is $5\times 10^{12}/cm^2$ and the polarization of optical wave is parallel to the wire axis. The corresponding radiative current density is 700 A/cm^2. For $\Delta p=0$ one broad spectrum is observed due to many closely spaced minibands. As Δp, hence confinement increases, one can clearly see the emergence of two gain peaks. The first peak corresponds to the transition from the first conduction miniband to the first valence miniband. The second peak indicated by arrows is due to the transition between the second conduction miniband and the second valence miniband. As vertical confinement increases, the separation between these two peaks increases, the first gain peak becomes narrower and higher at a given carrier density, and the second peak diminishes significantly. These improvements mean that one can obtain smaller threshold currents and narrower linewidths.

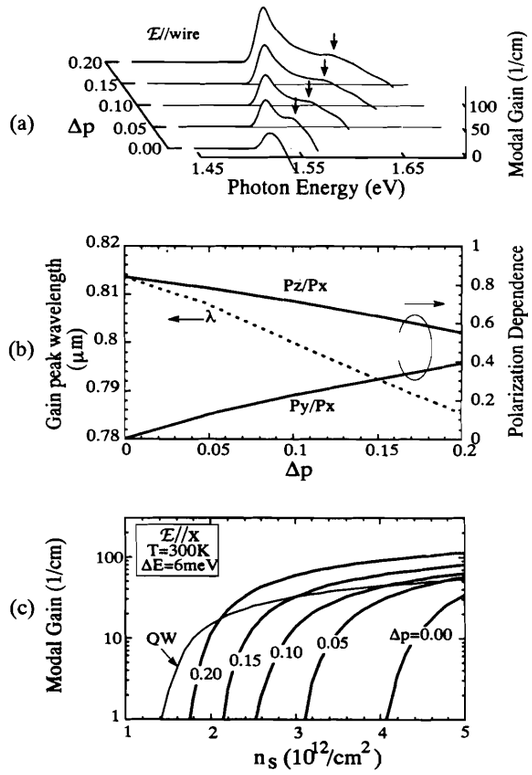

FIG. 3. Optical gain of a SSL with $x_b=x_c=0.50$, $W=S=54$ Å, $D_0=460$, $\Delta E=6$ meV, $T=300$ K, (a) modal gain spectrum at injected surface carrier density, $n_s=5\times 10^{12}/cm^2$ with electric field, $\mathscr{E}$, polarized along the wire axis. The arrows indicate the second gain peak. (b) Gain peak wavelength and polarization dependency of the peak gain. P_x, P_y, and P_z are the peak gains when the electric field is polarized in x, y, and z directions, respectively. (c) Maximum modal gain as a function of injected surface carrier density for different Δp values. Electric field is polarized along the wire axis. QW is a 54 Å thick single $GaAs/Al_{0.5}Ga_{0.5}As$ quantum well.

The peak gain when electric field polarization is in y and z directions, P_y and P_z, relative to the peak gain for x polarization, P_x, is plotted in Fig. 3(b) as a function of Δp. On this figure, the wavelength at which peak gain of x polarization occurs is also plotted. For $\Delta p=0$ the resulting structure is almost like a lateral quantum well array, hence the gain for y polarization is very small. P_z/P_x is slightly less than unity due to the weak vertical confinement. As Δp

increases, peak gain for z polarization decreases and peak gain for y polarization increases because of increased vertical confinement. When Δp is 0.2 the maximum gain for z and y polarizations become close, because for this degree of confinement the effective size of the lowest mode in y and z directions become about the same. Therefore, the structure becomes similar to an array of quantum wires of the square cross-sectional profile. The lasing wavelength decreases as Δp increases, since the energy of the lowest energy eigenvalue becomes higher for stronger vertical confinement.

The maximum modal gain is also plotted in Fig. 3(c) as a function of the injected surface carrier density at different Δp values when the electric field is polarized along the wires. With increased vertical confinement, the surface carrier density for optical transparency decreases since the gap between minibands increases as shown in Figs. 2 and 3(a). This modal gain is also compared with that of a 54 Å thick $GaAs/Al_{0.5}Ga_{0.5}As$ single quantum well. The quantum confinement is such a quantum well is almost the same as lateral quantum confinement in the SSL, so the changes in the SSL properties relative to this quantum well is due to additional vertical confinement originating from the curvature and reflect the expected benefits from additional degree of confinement. For $\Delta p=0.20$, the transparency surface carrier density for the SSL is $1.8\times10^{12}/cm^2$ and for the QW, $1.4\times10^{12}/cm^2$. Although, the transparency surface carrier density of QWR is slightly larger than that of QW, the differential gain and maximum modal gain of QWR are much larger than QW.

Just like any fabricated structure, SSL also deviates from the ideal structure considered so far. Presently the main problem in the SSL fabrication seems to be the incomplete segregation of the Al between the barrier region and wire regions.[15,16] If some of the Al intended to be in the barrier is incorporated in the wire region, the potential difference between barriers and wires decreases and consequently the lateral confinement becomes weak. This reduces lateral confinement and results in miniband broadening due to wire to wire coupling. There is also additional broadening due to other imperfections. However, based on our calculations on TSL in the case of weak lateral confinement the additional broadening due to other imperfections is insignificant.[17] We expect a similar conclusion for the SSL. Therefore, imperfect Al segregation is the main problem presently. This effect is studied by using a model which assumes that the average Al concentration in the lateral superlattice region remains constant at $x=0.25$. Assuming equal wire and barrier widths, this means $(x_b+x_w)/2=0.25$. Furthermore, the degree of segregation is defined as $\Delta x=x_b-x_w$ and it is assumed that Al composition varies abruptly between x_b and x_w. Figure 4 shows the maximum gain of a SSL grown on a 1.5° off substrate for different segregation or Δx. As Δx decreases the maximum modal gain decreases due to the reduced lateral confinement which increases the coupling between wires. A dramatic gain reduction can be seen when Δx is reduced from 0.4 to 0.3. When Δx is smaller than 0.3, the maximum gain is even smaller than that of the single QW. Furthermore, as

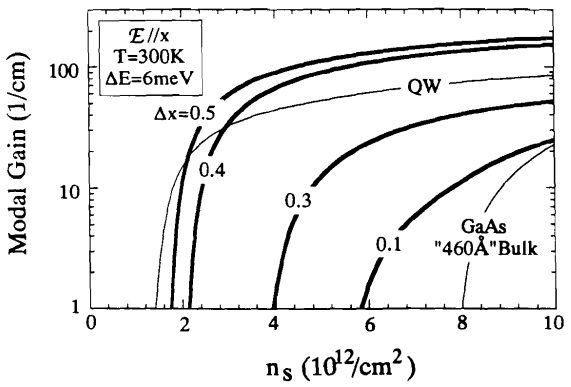

FIG. 4. Maximum gain of a SSL as a function of Al segregation, $\Delta x=x_b-x_w$ with $(x_b+x_w)/2=0.25$, $\Delta p=0.20$, $D_0=460$ Å, $W=S=54$ Å. QW is a 54 Å thick single $GaAs/Al_{0.5}Ga_{0.5}As$ quantum well. GaAs "460 Å" bulk is identical to the SSL structure except the SSL region is replaced by bulk GaAs.

the x_w increases, the separation between Γ and L valley subband minima decreases, increasing carrier leakage. Therefore, to observe enhanced room temperature gain properties compared to QW, the lateral Al segregation should be greater than 0.3.

In conclusion, the gain characteristics of serpentine superlattice quantum wire arrays grown on GaAs vicinal substrates were calculated including the valence band intermixing and miniband broadening effects. The effect of the imperfect Al segregation in the structure, which presently seems to be the main problem, was also investigated. Significant improvements in maximum and differential gain as well as in transparency carrier densities are expected provided that good Al segregation is realized.

Authors acknowledge the support of NSF through QUEST, the NSF Science and Technology Center on Quantized Electronic Structures at University of California, Santa Barbara, Grant No. DMR91-20007.

[1] D. S. Citrin and Y.-C. Chang, J. Appl. Phys. **68**, 161 (1990).
[2] P. C. Sercel and K. J. Vahala, Appl. Phys. Lett. **57**, 545 (1990).
[3] I. Suemune and L. A. Coldren, IEEE J. Quantum Electron. **QE-24**, 1778 (1988).
[4] C. Pryor, Phys. Rev. B **44**, 12912 (1991).
[5] P. M. Petroff, A. C. Gossard, and W. Wiegmann, Appl. Phys. Lett. **45**, 620 (1984).
[6] T. Fukui and H. Saito, Appl. Phys. Lett. **50**, 824 (1987).
[7] J. M. Gaines, P. M. Petroff, H. Kroemer, R. J. Simes, R. S. Geels, and J. H. English, J. Vac. Sci. Technol. B **6**, 1378 (1988).
[8] M. Tsuchiya, J. M. Gaines, R. H. Yan, R. J. Simes, P. O. Holtz, L. A. Coldren, and P. M. Petroff, Phys. Rev. Lett. **62**, 466 (1989).
[9] M. Asada, Y. Miyamoto, and Y. Suematsu, Jpn. J. Appl. Phys. **24**, L95 (1985).
[10] Y. Arakawa, K. Vahara, A. Yariv, and K. Lau, Appl. Phys. Lett. **47**, 1142 (1985).
[11] D. L. Crawford, R. L. Nagarajan, and J. E. Bowers, Appl. Phys. Lett. **58**, 1629 (1991).
[12] M. S. Miller, C. E. Pryor, H. Weman, L. A. Samoska, H. Kroemer, P. M. Petroff, and J. L. Merz, J. Cryst. Growth **111**, 323 (1991).
[13] T. Ando, S. Wakahara, and H. Akera, Phys. Rev. B **40**, 11609 (1989).
[14] J. M. Luttinger and W. Kohn, Phys. Rev. **97**, 869 (1955).
[15] T. Fukui, H. Saito, and Y. Tokura, Appl. Phys. Lett. **55**, 1958 (1989).
[16] M. S. Miller, H. Weman, C. E. Pryor, M. Krishnamurthy, P. M. Petroff, H. Kroemer and J. L. Merz, Phys. Rev. Lett. **68**, 3464 (1992).
[17] J. C. Yi, N. Dagli, and L. Coldren, Appl. Phys. Lett. **59**, 3015 (1991).